Trajectories of brain and hippocampal atrophy in FTD with mutations in *MAPT* or *GRN*

J.L. Whitwell, PhD
S.D. Weigand, MS
J.L. Gunter, PhD
B.F. Boeve, MD
R. Rademakers, PhD
M. Baker, BS
D.S. Knopman, MD
Z.K. Wszolek, MD
R.C. Petersen, MD, PhD
C.R. Jack, Jr., MD
K.A. Josephs, MD, MST, MSc

Address correspondence and reprint requests to Dr. Jennifer L. Whitwell, Department of Radiology, Mayo Clinic, 200 First St. SW, Rochester, MN 55905
Whitwell.jennifer@mayo.edu

ABSTRACT

Objective: To use multiple serial MRI to assess rates and trajectories of brain and hippocampal atrophy in subjects with frontotemporal dementia (FTD) with progranulin (*GRN*) or microtubule-associated protein tau (*MAPT*) gene mutations.

Methods: In this case-control study, we identified 8 subjects with mutations in *GRN* and 12 subjects with mutations in *MAPT* who had at least 2 serial MRIs. Serial MRIs were registered to baseline MRI for each subject using 9 *df* registration and rate of whole brain atrophy was calculated using the boundary-shift integral. Hippocampal volume was measured using Freesurfer. Mixed effects linear regression models were used to model volume change over time in both groups after adjusting for head size, age at baseline, and disease duration at baseline.

Results: The annual rate of whole brain atrophy in the *MAPT* subjects was 2.4% per year (95% confidence interval [CI] 1.9–2.8). The *GRN* subjects showed a higher rate of whole brain atrophy at 3.5% per year (95% CI 2.8–4.2; $p = 0.01$). Rates of hippocampal atrophy were not different across the groups (*MAPT* = 7.8% [95% CI 3.9–12], *GRN* = 6.5% [95% CI 1.7–11], $p = 0.66$). Rates of whole brain atrophy in *GRN*, and hippocampal atrophy in *MAPT*, were associated with age, with older subjects showing slower rates of atrophy ($p = 0.01$ and $p < 0.001$).

Conclusions: Subjects with FTD with *GRN* mutations have a faster rate of whole brain atrophy than subjects with FTD with *MAPT* mutations, with similar rates of hippocampal atrophy. Rates of atrophy in both groups were associated with age. These findings are important for future treatment trials in FTD that use rates of atrophy as an outcome measure. ***Neurology*® 2011;77:393–398**

GLOSSARY

BSI = boundary-shift integral; **CI** = confidence interval; **FTD** = frontotemporal dementia; **TIV** = total intracranial volume.

Frontotemporal dementia (FTD) is a progressive neurodegenerative disease associated with brain atrophy.[1,2] Rate of atrophy is an excellent disease biomarker that is already used as an outcome measure in treatment trials for neurodegenerative disorders other than FTD, since clinical trial data for FTD are sparse. Subjects with genetic mutations are ideal candidates for treatment trials in FTD since we can infer the underlying pathology. The 2 most commonly mutated genes in FTD are microtubule-associated protein tau (*MAPT*) and progranulin (*GRN*), with *MAPT* mutations associated with tau pathology and *GRN* mutations associated with TDP-43 pathology. Determining rate of atrophy in these 2 mutations, and understanding the natural biology of how brain volume changes over time, will be critical if rates of atrophy are to be utilized as outcome measures in future treatment trials using these subjects.

The aim of this study was to assess rates and trajectories of whole brain and hippocampal atrophy throughout the disease course in subjects with these mutations. Given the variability in age at onset and large differences between *GRN* and *MAPT* mutations,[3] we also assessed whether rate of atrophy is associated with age.

From the Departments of Radiology (J.L.W., C.R.J.), Biostatistics (S.D.W.), Information Technology (J.L.G.), and Neurology (B.F.B., D.S.K., R.C.P., K.A.J.), Mayo Clinic, Rochester, MN; and Departments of Neuroscience (R.R., M.B.) and Neurology (Z.K.W.), Mayo Clinic, Jacksonville, FL.

Study funding: Supported by the NIH (R01-DC010367, R01-AG037491, R21-AG38736, R01-AG11378, P50-AG16574, R01-NS065782, P50-NS072187, and R01-AG02651). Support for several investigators was provided by the Robert H. and Clarice Smith and Abigail Van Buren Alzheimer's Disease Research Program of the Mayo Foundation and the NIH Construction Grant (C06 RR018898).

Disclosure: Author disclosures are provided at the end of the article.

Table Subject demographics[a]

	GRN control (n = 8)	*GRN* (n = 8)	*MAPT* control (n = 12)	*MAPT* (n = 12)
No. (%) female	6 (75)	5 (63)	5 (38)	6 (50)
Education, y	14 (12 to 16)	14 (12 to 16)	16 (12 to 20)	12 (12 to 18)
Age at onset, y[b]	NA	59 (55 to 83)		46 (24 to 60)
Age at baseline scan, y[b]	60 (57 to 84)	60 (57 to 83)	55 (42 to 63)	49 (25 to 62)
Disease duration, y	NA	4 (2 to 6)		6 (2 to 15)
STMS at baseline scan	36 (32 to 37)	29 (21 to 32)[c]	37 (35 to 38)	32 (24 to 36)[d]
MMSE at baseline scan	30 (29 to 30)	24 (15 to 27)[c]	30 (27 to 30)	29 (23 to 30)[d]
CDR-SB at baseline scan	0 (0 to 0)	4.5 (0.5 to 18)[c]	0 (0 to 0)	1.5 (0 to 9)[d]
No. of MRI for whole brain volume	2 (2 to 3)	3 (2 to 5)	4 (2 to 5)	4 (2 to 14)
No. of MRI for hippocampal volume	2 (2 to 3)	3 (2 to 4)	4 (2 to 5)	3 (2 to 8)
Years from first to last MRI	2 (2 to 3)	2 (1 to 4)	4 (2 to 14)	4 (1 to 9)
Baseline brain volume, L	1.38 (1.11 to 1.52)	1.14 (1.04 to 1.38)[c]	1.41 (1.24 to 1.78)	1.35 (0.97 to 1.63)
Baseline hippocampal volume, cm^3	8.04 (7.33 to 9.93)	6.40 (5.85 to 7.25)[c]	9.05 (7.79 to 9.85)	5.88 (4.27 to 8.35)[d]
Rate of whole brain atrophy, %/y (95% CI)[b]	0.2 (0.1 to 0.5)	3.5 (2.8 to 4.2)[c]	0.2 (0.1 to 0.4)	2.4 (1.9 to 2.8)[d]
Rate of hippocampal atrophy, %/y (95% CI)	0.5 (−0.5 to 1.5)	6.5 (1.7 to 11)[c]	0.0 (−0.3 to 0.3)	7.8 (3.9 to 12)[d]

Abbreviations: CDR-SB = Clinical Dementia Rating Scale Sum of Boxes; CI = confidence interval; MMSE = Mini-Mental State Examination; STMS = Short Test of Mental Status.
[a] Unless otherwise indicated, values shown are median (range). Disease duration is calculated as time from onset to first MRI. Five subjects in *GRN* controls, 3 subjects in *GRN*, 4 subjects in *MAPT* controls, and 4 subjects in *MAPT* had only 2 serial MRI.
[b] Significant difference observed between the *GRN* and *MAPT* groups at $p < 0.05$.
[c] Significant difference observed between *GRN* and *GRN* controls at $p < 0.05$.
[d] Significant difference observed between *MAPT* and *MAPT* controls at $p < 0.05$.

METHODS

Subjects. We identified all subjects from Mayo Clinic, MN, between January 1992 and January 2011 who had screened positive for mutations in *GRN* or *MAPT* and had at least 2 MRIs. All subjects were followed prospectively with annual clinical examinations. Eight *GRN* subjects (5 families) were identified, with 5 mutations: 4 subjects with the c.154delA(p.Thr52HisfsX2) mutation, and one subject each with mutations c.1477C>T(p.Arg493X), c.102delC(p.Gly35GlufsX19), c.1145delC(p.Thr382SerfsX30), and c.138 + 1G>A(IVS1 + 1G>A p.Met). Twelve *MAPT* subjects (9 families) were identified, with 6 mutations: 4 subjects with P301L [c.1907C>T(p.Pro301Leu)], 2 subjects with S305N [c.1919G>A (p.Ser305Asn)], 2 subjects with 10 + 3 [c.1920 + 3G>A (IVS10 + 3G>A)], 2 subjects with 10 + 16 [c.1920 + 16C>T(IVS10 + 16C>T)], and one subject each with N279K [c.1842T>G(p.Asn279Lys)] and G389R [c.2170G>A(p.Gly389Arg)] mutations. Six *GRN* and 2 *MAPT* subjects came to autopsy showing TDP-43 immunoreactive inclusions in the former group, and widespread tau deposition in the later. Detailed clinical data have been previously reported in these cases.[4,5] The *GRN* and *MAPT* groups were each matched to a healthy control cohort by age, gender, number of MRI, and time from first to last MRI. Subject demographics are shown in the table.

Standard protocol approvals. Informed consent was obtained from all subjects for participation in the studies, which were approved by the Mayo institutional review board.

MRI analysis. All MRI were acquired using standardized imaging protocols. Thirteen subjects were scanned at 1.5 T, 4 subjects at 3 T, and 3 subjects had early scans performed at 1.5 T and later scans performed at 3 T. All MRI underwent preprocessing correction for gradient nonlinearity and intensity nonuniformity. To generate whole brain data, serial MRI were registered to baseline for each subject using 9 *df* registration. All registrations were performed across scan pairs performed at the same field strength. Hence, 3 T scans were registered to the first available 3 T scan. Change in brain volume was calculated from registered scan pairs using the boundary-shift integral (BSI).[6] The BSI results between each interval were used to calculate brain volume at each timepoint. Hippocampal and total intracranial volume (TIV) were calculated for each timepoint using the Freesurfer software (version 4.5.0)[7] longitudinal pipeline. Freesurfer processing was only performed on batches of serial scans performed at the same field strength.

Statistics. Mixed-effects linear regression models using disease duration at baseline as the time scale were used to estimate change in brain volume over time among *MAPT* and *GRN* subjects. Random kindred and subject-within-kindred intercepts and slopes were included. Fixed effects of primary interest were disease duration, genotype, and a disease duration–by–genotype interaction. The model also included fixed effects for field strength, TIV, and age at baseline MRI. Together, these fixed effects allow brain volume to decline linearly with disease duration with possibly different rates of decline by genotype. We modeled the log of brain volume to estimate rate of volume loss expressed as percentage per year. To evaluate the effect of age separately within genotype, we fitted a model that included a 3-way interaction between genotype, disease duration, and age at baseline MRI. We used a similar approach to compare cases to their respective control groups but omitted kindred from the models and by necessity treated time from baseline MRI as the

Figure 1 Trajectories of whole brain volume loss in *GRN* and *MAPT*

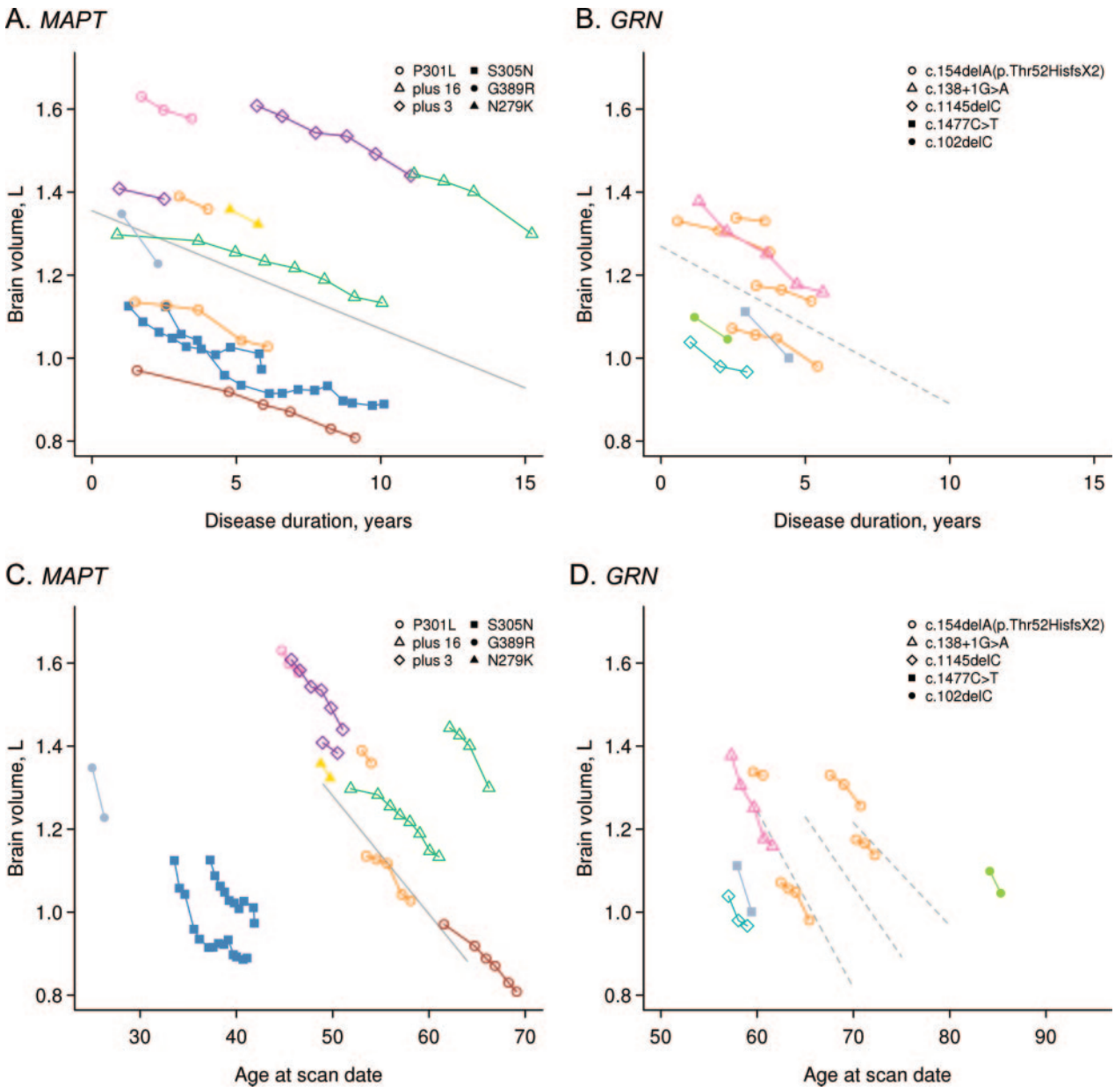

(A, B) Whole brain volume plotted against disease duration. (C, D) Whole brain volume plotted against age at scan. Data points for individual subjects are shown with the different colors representing different genetic families. The legend highlights the specific mutations of each subject. Volume estimates from 3 T scans are adjusted downward by 0.031 L to remove slight field-strength effects. The solid line in A represents the average volume as a function of disease duration for *MAPT* subjects assuming age at baseline of 49 years, disease duration at baseline of 1.6 years, and total intracranial volume (TIV) of 1.44 L, the median values in the group. The dashed line in B represents the average volume for *GRN* subjects assuming age at baseline of 61 years, duration at baseline of 1.9 years, and TIV of 1.40 L, the median values in the group. The solid line in C represents average volume for *MAPT* subjects as a function of age assuming age at baseline of 49 years, disease duration at baseline of 1.6 years, and TIV of 1.44 L. The dashed lines in D contrast average volume for *GRN* subjects as a function of age comparing subjects with baseline ages of 60, 65, and 70 years, assuming duration at baseline of 1.9 years and TIV of 1.40 L.

timescale. Because subject measurements were observed to be approximately linear over the observed time period and because of the few subjects, in order to protect against overfitting, we made the simplifying assumption of linear within-subject trajectories.

RESULTS The annual rate of whole brain atrophy was higher in both *GRN* and *MAPT* compared to controls ($p < 0.001$ for both), with rates higher in *GRN* compared to *MAPT* ($p = 0.01$) (table and figure 1). The estimated annual rate of hippocampal atrophy was also higher in both *GRN* and *MAPT* compared to controls ($p < 0.001$ for both), although no difference was observed between *GRN* and *MAPT* ($p = 0.66$) (table and figure 2).

Figure 2 Trajectories of hippocampal volume loss in *GRN* and *MAPT*

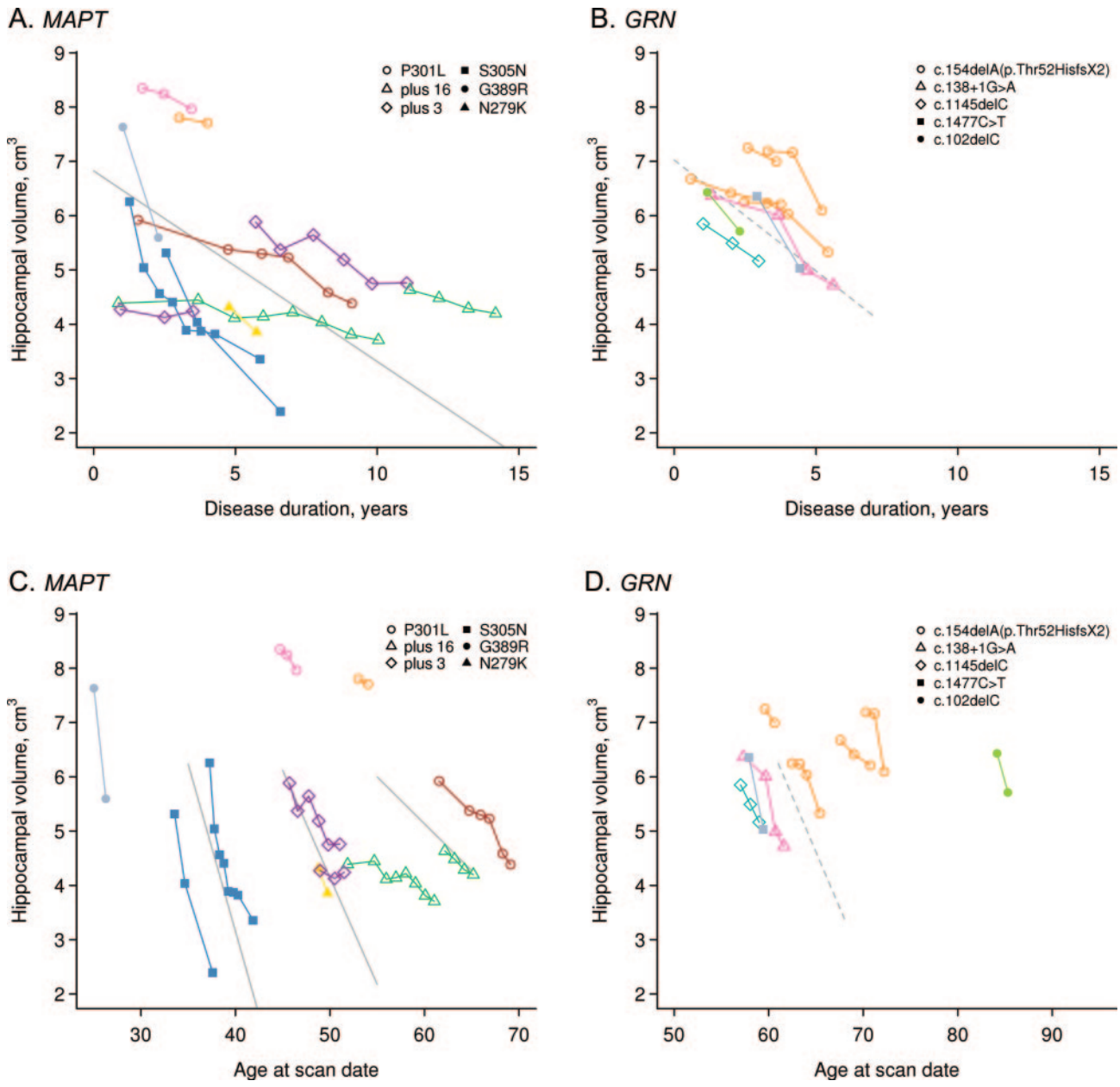

(A, B) Hippocampal volume plotted against disease duration. (C, D) Hippocampal volume plotted against age at scan. Data points for individual subjects are shown with the different colors representing different families. The legend highlights the specific mutations of each subject. Volume estimates from 3 T scans are adjusted downward by 0.036 cm^3 to remove slight field-strength effects. The solid line in A represents the average volume as a function of disease duration for *MAPT* subjects assuming age at baseline of 49 years, disease duration at baseline of 1.6 years, and total intracranial volume (TIV) of 1.44 L, the median values in the group. The dashed line in B represents the average volume for *GRN* subjects assuming age at baseline of 61 years, duration at baseline of 1.9 years, and TIV of 1.40 L, the median values in the group. The solid lines in C contrast average volume for *MAPT* subjects as a function of age comparing subjects with baseline ages of 35, 45, and 55 years, assuming duration at baseline of 1.6 years and TIV of 1.44 L. The dashed line in D represents average volume for *GRN* subjects as a function of age assuming duration at baseline of 1.9 years and TIV of 1.40 L.

Rates of whole brain atrophy in the *GRN* group differed according to age ($p = 0.01$), with older subjects showing slower rates of atrophy (i.e., rates at age 60 = 3.7%/year, 65 = 2.9%, and 70 = 2.1%/year) (figure 1). In contrast, rates of hippocampal atrophy in the *MAPT* group differed according to age ($p < 0.001$), with older subjects showing slower rates of atrophy (i.e., rates at age 35 = 13.6%/year, 45 = 8.6%/year, and 55 = 3.6%/year) (figure 2). No effect of age was observed on rates of hippocampal atrophy in *GRN* ($p = 0.86$) and whole brain atrophy in *MAPT* ($p = 0.57$).

DISCUSSION Using multiple serial MRI scans and mixed effects modeling, we demonstrated that subjects with *GRN* mutations have a faster trajectory of

whole brain atrophy than subjects with *MAPT* mutations, suggesting a more rapidly progressing disease course in *GRN*. One other small study that assessed rates of atrophy using only 2 MRI scans per subject similarly found faster rates of atrophy in *GRN*.[8] Our finding is also in keeping with another study that demonstrated faster rates of functional decline in *GRN* compared to *MAPT*.[9] Rates of hippocampal atrophy were similar, however, across the mutations. Interestingly, the ratio of hippocampal to whole brain atrophy was greater in *MAPT* (3:1) than *GRN* (2:1), suggesting disproportionate involvement of the hippocampus in *MAPT*. Indeed, anteromedial temporal atrophy is a feature of *MAPT* mutations.[10]

In addition, rates of atrophy in *GRN* and *MAPT* were associated with age. In *GRN,* rates of whole brain atrophy were faster in younger than older subjects, and in *MAPT*, rates of hippocampal atrophy were faster in younger than older subjects. These findings may reflect the anatomic signatures of these mutations. Mutations in *GRN* are associated with widespread cerebral atrophy and so may be better represented by a whole brain measure of atrophy, whereas *MAPT* mutations are associated with anteromedial temporal atrophy which may be better represented by hippocampal measures. Since the *MAPT* subjects were younger than the *GRN* subjects, as previously reported,[3,5] yet had slower rates of whole brain atrophy, our findings suggest that the age effect occurs within each mutation group and not across all subjects with genetic mutations.

Based on our models, we found a significant field-strength effect ($p = 0.003$) with 3 T scans showing larger volume estimates. However, we accounted for these differences in our analysis and found that field strength was not associated with group ($p = 0.78$). The number of serial MRIs was lower in the *GRN* group, which could have reduced power, although we were still able to identify a significant age effect in this group. These findings highlight important differences across *GRN* and *MAPT* subjects which will be important for future treatment trials that employ rates of atrophy as biomarkers.

AUTHOR CONTRIBUTIONS

Dr. Whitwell: drafting/revising the manuscript for content, study concept or design, analysis or interpretation of the data. S.D. Weigand: drafting/revising the manuscript for content, analysis or interpretation of the data, statistical analysis. Dr. Gunter: drafting/revising the manuscript for content, analysis or interpretation of the data. Dr. Boeve: drafting/revising the manuscript for content, acquisition of data. Dr. Rademakers: drafting/revising the manuscript for content, acquisition of data. M. Baker: drafting/revising the manuscript for content, acquisition of data. Dr. Knopman: drafting/revising the manuscript for content, acquisition of data. Dr. Wszolek: drafting/revising the manuscript for content, acquisition of data, obtaining funding. Dr. Petersen: drafting/revising the manuscript for content, acquisition of data, obtaining funding. Dr. Jack: drafting/revising the manuscript for content, acquisition of data, obtaining funding. Dr. Josephs: drafting/revising the manuscript for content, study concept or design, analysis or interpretation of the data, acquisition of data, study supervision.

ACKNOWLEDGMENT

The authors thank Dr. Dennis Dickson and Dr. Joseph Parisi for pathologic evaluations.

DISCLOSURE

Dr. Whitwell receives research support from the NIH and the Dana Foundation. S.D. Weigand and Dr. Gunter report no disclosures. Dr. Boeve has served as a consultant to GE Healthcare; receives publishing royalties for *The Behavioral Neurology of Dementia* (Cambridge University Press, 2009); and receives research support from Cephalon, Inc., Allon Therapeutics, Inc., the NIH/NIA, the Alzheimer's Association, and the Mangurian Foundation. Dr. Rademakers holds patents re: Methods and materials for detecting and treating dementia and receives research support from the NIH, the Pacific Alzheimer Research Foundation (Canada), the Association for Frontotemporal Dementia, the Amyotrophic Lateral Sclerosis Association, CurePSP, and the Consortium for Frontotemporal Dementia. M. Baker holds patents re: Methods and materials for detecting and treating dementia. Dr. Knopman serves as Deputy Editor for *Neurology*®; has served on a data safety monitoring board for Eli Lilly and Company; has served as a consultant for Elan/Janssen AI; is an investigator in clinical trials sponsored by Elan/Janssen AI, Baxter International Inc., and Forest Laboratories, Inc.; and receives research support from the NIH. Dr. Wszolek serves as Co-Editor-in-Chief of *Parkinsonism and Related Disorders*, Regional Editor of the *European Journal of Neurology*, and on the editorial boards of *Neurologia i Neurochirurgia Polska*, *Advances in Rehabilitation*, the *Medical Journal of the Rzeszow University*, and *Clinical and Experimental Medical Letters*; holds and has contractual rights for receipt of future royalty payments from patents re: A novel polynucleotide involved in heritable Parkinson's disease; receives royalties from publishing *Parkinsonism and Related Disorders* (Elsevier, 2007, 2008, 2009) and the *European Journal of Neurology* (Wiley-Blackwell, 2007, 2008, 2009); and receives research support from Allergan, Inc., the NIH, the Pacific Alzheimer Research Foundation (Canada), the CIHR, the Mayo Clinic Florida Research Committee CR program, and a gift from Carl Edward Bolch, Jr., and Susan Bass Bolch. Dr. Petersen serves on scientific advisory boards for the Alzheimer's Association, the National Advisory Council on Aging (NIA), Elan/Janssen AI, Pfizer Inc (Wyeth), and GE Healthcare; receives royalties from publishing *Mild Cognitive Impairment* (Oxford University Press, 2003); serves as a consultant for Elan/Janssen AI and GE Healthcare; and receives research support from the NIH/NIA. Dr. Jack serves on scientific advisory boards for Elan/Janssen AI, Eli Lilly & Company, GE Healthcare, and Eisai Inc.; receives research support from Baxter International Inc., Allon Therapeutics, Inc., Pfizer Inc, the NIH/NIA, and the Alexander Family Alzheimer's Disease Research Professorship of the Mayo Foundation; and holds stock/stock options in Johnson & Johnson. Dr. Josephs receives research support from the NIH (NIDCD, NIA) and the Dana Foundation.

Received December 20, 2010. Accepted in final form April 5, 2011.

REFERENCES

1. Chan D, Fox NC, Jenkins R, et al. Rates of global and regional cerebral atrophy in AD and frontotemporal dementia. Neurology 2001;57:1756–1763.
2. Whitwell JL, Jack CR Jr, Parisi JE, et al. Rates of cerebral atrophy differ in different degenerative pathologies. Brain 2007;130:1148–1158.
3. Pickering-Brown SM, Rollinson S, Du Plessis D, et al. Frequency and clinical characteristics of progranulin

mutation carriers in the Manchester frontotemporal lobar degeneration cohort: comparison with patients with MAPT and no known mutations. Brain 2008;131:721–731.
4. Kelley BJ, Haidar W, Boeve BF, et al. Prominent phenotypic variability associated with mutations in Progranulin. Neurobiol Aging 2009;30:739–751.
5. Whitwell JL, Jack CR Jr, Boeve BF, et al. Voxel-based morphometry patterns of atrophy in FTLD with mutations in MAPT or PGRN. Neurology 2009;72:813–820.
6. Gunter JL, Shiung MM, Manduca A, Jack CR Jr. Methodological considerations for measuring rates of brain atrophy. J Magn Reson Imaging 2003;18:16–24.
7. Fischl B, Dale AM. Measuring the thickness of the human cortex from magnetic resonance images. Proc Nat Acad Sci USA 2000;97:11050–11055.
8. Rohrer JD, Ridgway GR, Modat M, et al. Distinct profiles of brain atrophy in frontotemporal lobar degeneration caused by progranulin and tau mutations. NeuroImage 2010;53:1070–1076.
9. Josephs KA Jr, Whitwell JL, Weigand SD, et al. Predicting functional decline in behavioral variant frontotemporal dementia. Brain 2011;134:432–448.
10. Whitwell JL, Jack CR Jr, Boeve BF, et al. Atrophy patterns in IVS10+16, IVS10+3, N279K, S305N, P301L, and V337M MAPT mutations. Neurology 2009;73:1058–1065.